

Design of Wide-Temperature Lithium-Sulfur Batteries

Hang Yang,^[a] Yangmingyue Zhao,^[a] Suo Li,^[a] Hao Tong,^[a] and Libo Li^{*[a]}

In electrochemical energy storage (EES), lithium-sulfur (Li–S) batteries have recently gained recognition for their exceptional theoretical specific capacity, making them stand out among a wide range of cutting-edge energy storage technologies. While Li–S batteries demonstrate a long cycle life under regular conditions, expanding their application scenarios is crucial for their future development. Specifically, ensuring stable battery operation in extreme temperature environments, such as below

0 °C and above 60 °C, becomes paramount. Thus, this review aims to summarize the recent progress of Li–S batteries in extreme temperature ranges and analyse the processability of critical materials within these batteries at extreme temperatures. Ultimately, this review presents insights and potential prospects for Li–S battery systems operating within a wide temperature range, contributing to advancing energy storage devices capable of functioning across various temperatures.

1. Introduction

The international community has rapidly shifted to renewable energy sources to mitigate the irreversible damage caused by increased carbon dioxide emissions.^[1–5] However, to maximize the benefits of renewable energy sources and reduce our overall carbon emissions, developing and using cutting-edge energy technologies is one of the current research centers.^[6–11] Lithium metal, with its high theoretical capacity (3860 mAh g⁻¹) and lowest redox potential, is one of the most promising anode materials for advanced batteries with high energy density.^[12–14] Among other things, the energy density of the ubiquitous lithium-ion battery is rapidly approaching its theoretical limit. To surpass this limit, a promising strategy is replacing conventional intercalation-type materials with conversion-type sulfur electrodes with higher energy, where the sulfur anode provides a higher theoretical specific capacity than the intercalation-type Li-ion battery.^[15–17] Therefore, lithium-sulfur (Li–S) batteries are the most attractive next-generation rechargeable energy storage device. Despite these advantages of Li–S batteries, which currently provide long life under conventional conditions, wide-temperature lithium batteries are one of the most advanced technologies on the market today.^[18–26] The cooperation of lithium technology and wide temperature range makes this battery type suitable for various applications. Among them, wide-temperature Li–S batteries have extensive practical applications in different environments, covering polar science, military applications, automotive, and transportation. These batteries provide reliable power in extreme temperature conditions, ensuring proper operation of equipment and systems.^[27] The charging temperature range of wide-temperature batteries is between –20 °C ~60 °C.^[28] Owing to the diversity of climate required to extend the working temperature limit of lithium batteries to below –50 °C or above 100 °C to

meet the operation of more extreme electronic equipment (underground or space exploration).^[29] However, current Li–S batteries operating at low or high temperatures usually deteriorate the electrochemical performance and even lead to thermal runaway, severely limiting the application of wide-temperature Li–S batteries.^[30] Therefore, exploring the failure mechanisms of wide-temperature Li–S batteries and how to adapt to extreme conditions is currently an attractive challenge. At low temperatures, the loss of capacity in Li–S batteries is due to the slow redox kinetics caused by the aggregation and deposition of lithium polysulfide clusters, which passivates the electrode surfaces and further hampers the transfer of carriers.^[31] At high temperatures, conventional ether electrolytes used in Li–S batteries have low boiling and flash points, which do not meet the demands of battery operation at high temperatures. At the same time, the high-temperature working environment will accelerate the dissolution of lithium polysulfide in the electrolyte, which will lead to a severe “shuttle effect”. Based on the above issues, modifying the electrode materials, electrolytes, and anodes of Li–S batteries in a wide temperature range is critical. As shown in Figure 1, representative materials in the research progress and current material design strategies are listed to understand the material progress fully. In this review, we outline the latest developments of wide-temperature Li–S batteries, including inherent problems of flammability, poor low-temperature performance, and explosion, and illustrate the difficulties of Li–S batteries at different temperatures. Finally, some perspectives on the future research and development wide-temperature of Li–S batteries are provided.

2. Main Progress for Low-Temperature Performance of Lithium-Sulfur Batteries

With the increasing awareness of the energy crisis, the need for electric vehicles to reduce the burning of fossil fuels has aroused people's attention to the development of new energy systems.^[32] Although lithium-sulfur batteries at room temper-

[a] H. Yang, Y. Zhao, S. Li, H. Tong, Prof. L. Li
School of Materials Science and Chemical Engineering
Harbin University of Science and Technology
Harbin 150040, China
E-mail: libo@hrbust.edu.cn

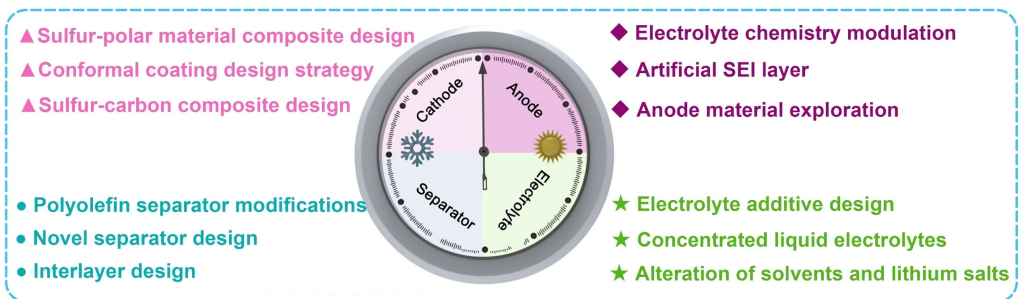


Figure 1. Current material design strategies for wide-temperature lithium-sulfur batteries.

ature with excellent cycle performance and alleviating the shuttle effect have been extensively studied, few studies have focused on the low-temperature performance of lithium-sulfur batteries.^[33] In particular, the demand for rechargeable batteries with increased energy density at sub-zero temperatures is rising, especially for drones and portable devices in harsh environments such as high altitudes and northeastern regions. Therefore, we summarize the progress of low-temperature lithium-sulfur literature in recent years.^[34]

2.1. Electrolyte

As an essential component of lithium-ion batteries, electrolytes not only determine the migration rate of Li^+ in the liquid phase but also participate in the formation of SEI film, which plays a vital role in the performance of solid-electrolyte interface (SEI) film.^[35] The viscosity of the electrolyte increases at low temperatures, the conductivity decreases, and the SEI film impedance increases, significantly deteriorating the battery's energy density and cycle performance. Currently, there are two ways to improve the low-temperature performance of electrolytes. 1) To improve the low-temperature conductivity of the electrolyte by



Hang Yang is currently a Ph.D. student at Harbin University of Science and Technology under the supervision of Prof. Libo Li. She received her master's degree from Qiqihar University in 2021. Her current research interests center on material design and mechanism investigation for Li-S batteries.



Hao Tong earned his bachelor's degree from Harbin University of Science and Technology. He is now a master student at Harbin University of Science and Technology under the supervision of Prof. Libo Li. His current research interests focus on Li metal anodes.



Yangmingyue Zhao is currently a Ph.D. student at Harbin University of Science and Technology under the supervision of Prof. Libo Li. Her current research interests center on the design and mechanism of polymer electrolytes and interfaces for Li-ion batteries.



Prof. Libo Li is a professor and doctoral supervisor of Materials Science and Chemical Engineering at Harbin University of Science and Technology. She received her Ph.D. degree from the Harbin Institute of Technology in 2006. Her research interests focus on advanced energy materials and storage batteries, including lithium-sulfur batteries, solid-state lithium batteries, lithium-ion batteries, and metal anodes.



Suo Li is currently a Ph.D. student at Harbin University of Science and Technology under the supervision of Prof. Libo Li. He received his master's degree from Guangxi University of Science and Technology in 2022. His research focuses on the design and synthesis of advanced electrode materials for high-performance Li-S batteries.

optimizing the composition of the solvent and using new electrolyte salts; 2) To use new additives to increase the conductivity of lithium ions at low temperatures.^[36]

In 2003, Yuriy et al.^[37] reported a new generation of lithium-sulfur rechargeable batteries based on specially designed electrolytes. The extraordinary experimental data of Li-S batteries in the low-temperature performance was worth noting. Their preliminary research shows that Li-S batteries still maintain better low-temperature rate performance under a high-voltage plateau; the low-voltage plateau rate and capacity were deeply affected by the temperature reduction. Excessive battery polarization on low-voltage platforms is the main obstacle to achieving low-temperature performance. In addition, the electrolyte type is a key factor affecting the polarization of low-platform batteries. Therefore, optimizing the electrolyte formulation and studying the influence of the different concentrations and different lithium salt solvents (LiSCN, LiSO₃CF₃, Li(N(SO₂CF₃)₂). Compared with high energy density Li-ion batteries (150 Wh kg⁻¹), Li-S systems with liquid cathodes having soluble sulfur and polysulfides demonstrated energy density exceeding 180 Wh kg⁻¹. This battery effectively prevents overcharging at low and room temperatures and lasts 30 times overcharging. To find the best electrolyte, Ryu et al.^[38] improved the low-temperature performance of Li-S batteries by adding 1, 3-dioxane and methyl acetate to the TEGDME electrolyte. At 20°C and -10°C, the first discharge capacity of the Li-S battery was 1303 mAh g⁻¹ and 357 mAh g⁻¹, respectively. The low temperature performance of Li/TEGDME/S battery was studied by means of discharge curve. Table 1 shows ionic conductivity and interfacial resistance at -10°C. The ionic conductivity of the TEGDME electrolyte is 8.1×10⁻⁵ S cm⁻¹, which is smaller than that at room temperature; the three different electrolytes show similar ionic conductivities. Although some people have previously studied the low-temperature performance of liquid electrolyte lithium-sulfur batteries, the low-temperature behaviors of Li-S cathodes have yet to be studied. There is a positive correlation between the Li⁺ desolvation energy barrier and the LiTFSI concentration in the electrolyte, and the Li⁺ desolvation process in the dilute electrolyte exhibits faster kinetics and improves the discharge capacity of lithium-sulfur batteries at low temperatures. Yan et al.^[39] weakened the Li⁺ desolvation energy barrier and enhanced the Li⁺ desolvation kinetic process of low-temperature Li-S batteries by decreasing the concentration of LiTFSI in the electrolyte, improving the electrochemical performance of low-temperature Li-S batteries. The discharge capacity of the Ah-grade Li-S soft pack battery fabricated with diluted electro-

lyte was about 1000 mAh g⁻¹ at 0°C, and the energy density was 350 Wh kg⁻¹.

2.2. Improved Cathode

The non-homogeneous redox reaction during charging/discharging at low temperatures is usually accompanied by slow reaction kinetics, which makes the multiplicative performance of lithium-sulfur batteries unsatisfactory. As for the low-temperature environment, the slow ion transport, low active substance utilization, and fast capacity decay at low temperature and the Li₂S accumulated on the electrode surface lead to the deterioration of the electrical conductivity. Therefore, many urgent problems remain to be solved in the research and development of high-performance, low-temperature lithium-sulfur batteries.^[40] Carbon materials have excellent physical, chemical, and mechanical properties. The weak polarity of pure carbon materials cannot inhibit polysulfide diffusion. To reduce the loss of active materials during the discharge process, heteroatom doping (N, S, P) has become an effective strategy for modulating the catalytic activity of carbon-based materials.^[41] The nitrogen and amino functional groups have a strong affinity for polysulfides. The doping of nitrogen atoms brings abundant active sites and improves the carbon conductivity to realize more practical lithium-sulfur batteries with excellent performance at low temperatures.^[42]

In 2016, Shaoyin et al.^[43] used nitrogen-enriched carbon and carbon/sulfur composite as raw materials to prepare the proper carbonization with the good low-temperature electrochemical performance. The electrochemical evaluation of the nitrogen-enriched carbon/sulfur composite cathode indicated that a reversible capacity of 368 mAh g⁻¹ (0.5 C) over 100 cycles was achieved at -20°C. The favorable electrochemical performance at low temperatures is attributed to the exceptional surface chemistry of nitrogen-enriched carbon materials with various amine groups, which enhances polysulfide immobilization. Additionally, long-chain polysulfides trapped in the carbon matrix through strong chemical absorption act as catalysts and react with insoluble charge products (Li₂S/Li₂S₂), transferring them to soluble intermediates and increasing low platform capacity. The major challenge in the practical implementation of lithium-sulfur batteries lies in long-chain polysulfides dissolved within organic electrolytes, which act as a "shuttle" between the electrodes and result in a rapid capacity decline. Chemical bonds modification can effectively stabilize graphene and improve the performance of Li-S batteries at room temperature and low temperature. In 2018, Zhang et al.^[44] synthesized a novel multifunctional complex of graphene oxide-Zn(II)-triazole (referred to as GO-Zn(II)-AmTZ), which exhibited exceptional performance at -20°C. The GO-Zn(II)-AmTZ cathode demonstrated a discharge capacity of 315 mAh g⁻¹ (0.5 C) after 100 cycles at -20°C. The performance has been enhanced through the improved immobilization of polysulfide on GO-Zn(II)-AmTZ, facilitated by the presence of Zn(II), amine groups, and N atoms. Furthermore, the cycle performance of carbon/sulfur composites was compared before

Table 1. Ionic conductivities and interfacial resistance of Li-S battery with various electrolyte such as TEGDME, TEG-DOX and DOXL at -10°C

Electrolyte	Ionic conductivity (S cm ⁻¹)	Interfacial resistance (Ω)
TEGDME	8.1×10 ⁻⁵	42120
TEGDME-DOXL	9.6×10 ⁻⁵	12320
DOXL	9.8×10 ⁻⁵	14630

and after modification with amine groups, nitrogen atoms, and zinc ions at low temperatures (-20°C). In the S@GO-Zn(II)-AmTZ, some active S on the outer layer of the cathode during the discharge process, while the soluble polysulfides can't rapidly diffuse back to the cathode due to the high viscosity of the electrolyte at -20°C , so the discharge capacity gradually decreases at the initial 10 cycles. The implication arises that the electrolyte's characteristic may serve as a pivotal factor in determining the electrochemical performance of the battery at low temperatures. Yu et al.^[45] prepared a self-supported three-dimensional porous material with embedded CoFe@C core-shell structure by high-temperature pyrolysis. CoFe bimetallic nanoparticles were able to catalyze the conversion of polysulfides. The self-supported three-dimensional porous material has good electrical conductivity, which provides an efficient ion/electron transport channel, alleviates the charge/discharge volume change, and avoids the large accumulation of Li_2S on the electrode surface. When the temperature drops below 0°C , most lithium-ion batteries cannot be charged and discharged properly due to the slow reaction kinetics. For the more complex reaction process of lithium-sulfur batteries, the low temperature has a more obvious effect on the performance of lithium-sulfur batteries. The electrochemical performance was tested at -10°C and -20°C , respectively. The charging and discharging curves clearly displayed two different discharge platforms, reflecting their good redox kinetics at low temperatures.

The concentration of lithium salt can significantly affect the performance of lithium-sulfur batteries because the concentration of lithium salt affects not only the dissolution and shuttle of Li_2S_x but also the formation of SEI film. However, most studies seldom explored the reasons for improving the battery performance from the perspective of solvation structures. Yan et al.^[46] prepared lithium-sulfur battery electrolytes with conventional solvent (DOL/DME, 1:1) and different concentrations of LiTFSI, comparing the low-temperature perform-

ance of electrolytes with concentrations. Li-S batteries with 0.5 M electrolyte retained 67.34% capacity at -40°C compared with 25 C. The lithium-sulfur pouch cell using a 0.5 M electrolyte achieved a high specific capacity of 1000 mAh g^{-1} at 0°C , which provides a promising avenue for the practical application of high-energy low-temperature lithium-sulfur batteries. The above studies confirmed a positive correlation between the Li^+ desolvation energy barrier and the LiTFSI concentration in the electrolyte. They improved the discharge capacity of lithium-sulfur batteries at low temperatures.

Wu et al.^[47] investigated the anodic sulfur conversion at low temperatures and improved the anodic reaction kinetics through low electrolyte concentration. There are the following three main effects: (1) lowering the lithium salt concentration can induce the Li_2S deposition mode to change from transient nucleation model to continuous nucleation, the deposited particles change from two-dimensional planar growth to island-like aggregation, the second discharge platform is prolonged, and the reversible capacity of the battery is improved; (2) lowering the lithium salt concentration can effectively weaken the effect of lithium polysulfide clustering, improve the migration number of lithium ions, and reduce the ion transfer impedance caused by the stacking of the lithium polysulfide. The ion transfer impedance caused by the bilayer is reduced, and the anode conversion kinetics is improved, which is conducive to the dense deposition of lithium metal, reducing the side reactions and improving the cycling stability of the batter. An electrolyte that simultaneously improves the performance of lithium metal and sulfur-based cathodes at extremely low temperatures is a major challenge (Figure 2a–e).

2.3. Functional Electrolyte Additive

The current research on low-temperature lithium-sulfur batteries is mainly improved based on ordinary Li-S batteries'

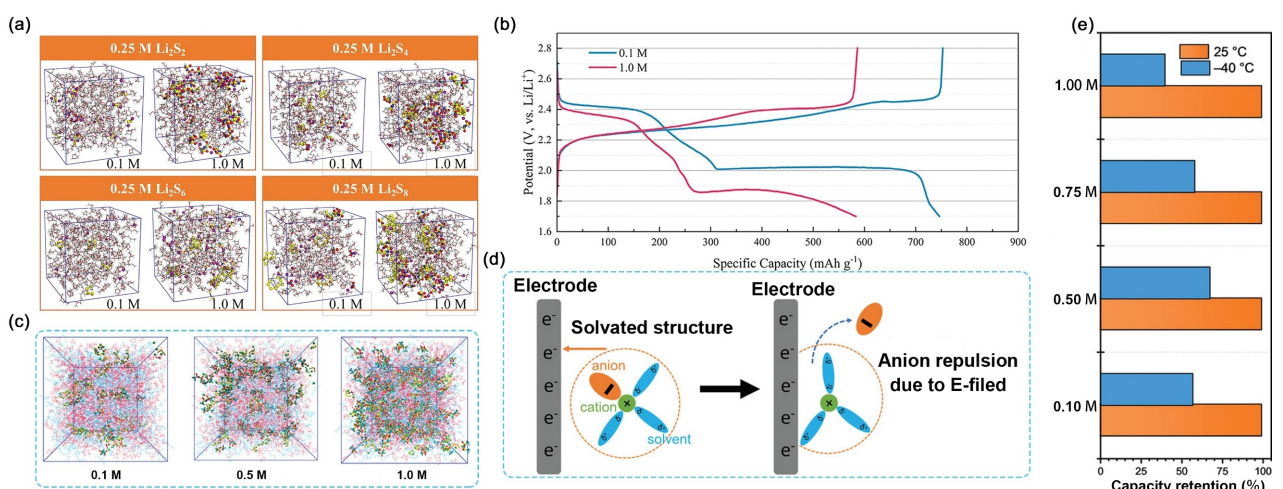


Figure 2. a) Computational atomicistic simulations of 0.1 and 1 M electrolyte with 0.25 M Li_2S_x at -20°C .^[47] b) Charge and discharge profiles of Li-S batteries using 0.1 and 1 M electrolyte discharging at -20°C and the corresponding resistances obtained by equivalent circuit.^[47] c) Snapshots obtained from MD simulations of electrolytes with different LiTFSI concentrations (0.1, 0.5, and 1.0 M).^[46] d) Scheme of the de-solvation process.^[46] e) The capacity retention rate of Li-S batteries with different electrolytes at -40°C .

electrolyte and electrode materials to achieve better low-temperature performance. At present, all solid-state electrolytes have high electrochemical performance and have commercial prospects. Solid-state lithium-sulfur batteries have shown promise as a safe, high-energy electrochemical storage technology to power regional electrified transportation. Owing to the limited ion mobility in crystalline polymer electrolytes, the batteries are unable to operate at sub-zero temperatures.^[48] Adding liquid plasticizers to the polymer electrolyte improves the conductivity of lithium ions at the expense of mechanical strength and interfacial stability with the two electrodes. In year 2020, Cai et al.^[49] developed a new ester-based electrolyte (LiFSI MP/FEC) as a Li-SPAN battery that can be cycled at ultra-low temperatures; when cycled at a current density of 0.1 A g^{-1} , Li || SPAN half cells retained over 91% and 78% of their room-temperature capacity at -20°C and -40°C , respectively (Figure 3a-b). Presently, research on the performance of low-temperature lithium-sulfur batteries is mainly focused on developing low-temperature electrolytes to increase the ionic conductivity of the electrolyte and reduce charge transfer resistance in current LIBs. Adding low melting point and low viscosity carboxylate-based co-solvents to mitigate the limitation of the high melting point of carbonate electrolytes on Li-SPAN batteries at low temperatures. However, these molecules react highly with lithium metal, leading to reducing cycle performance and dangerous dendrite growth, especially at frigid temperatures. Fluoride-donating additives improved the cycle performance of Li metal anodes; they also provided Li metal anodes with improved reversibility and sub-zero temper-

ature performance. This work enhanced the energy loss at sub-zero temperatures and provided a key design strategy for rechargeable batteries with high energy density at ultra-low temperatures. Wan et al.^[50] built an integrated dynamic cross-linked polymer network by introducing a spherical hyperbranched solid polymer plasticizer into the Li^+ conducting linear polymer matrix to remain completely amorphous over a wide temperature range from low 0°C (Figure 3c-d). Solid-state Li-S batteries with the novel electrolyte provide high reversible capacity and long cycle life at 25°C , 0°C and -10°C for energy storage under complex environmental conditions. Wu et al.^[51] designed a bimetallic amorphous polysulfide $\text{Mo}_{0.5}\text{Ti}_{0.5}\text{S}_4$ for operation at high multiplicity and low temperature. The introduction of Ti was beneficial in reducing the elastic modulus, thus accelerating the amorphization of crystalline MoS_2 during ball milling. On the other hand, the introduction of Ti facilitates the fabrication of more active sites and inhibited the segregation of S/Li₂S in the amorphous matrix. As a result, the specific capacity of $\text{Mo}_{0.5}\text{Ti}_{0.5}\text{S}_4$ was significantly increased from 757 to 914 mAh g^{-1} as compared to its counterpart, MoS_2 . The capacity retention of $\text{Mo}_{0.5}\text{Ti}_{0.5}\text{S}_4$ at a current rate of 4 C was increased from 47.2% to 65.8% owing to the improved diffusion kinetics and the surface-controlled (pseudocapacitance) contribution. In addition, the low-temperature performance of $\text{Mo}_{0.5}\text{Ti}_{0.5}\text{S}_4$ is also improved, with good long-cycle stability and multiplicity performance at -20°C (50.5% capacity retention at -20°C , 0.5 C) and capacity retention at -40°C , 0.1 C , from 35.1% to 50.7%. Therefore, $\text{Mo}_{0.5}\text{Ti}_{0.5}\text{S}_4$, with a bimetallic amorphous structure and rich in sulfur anions is

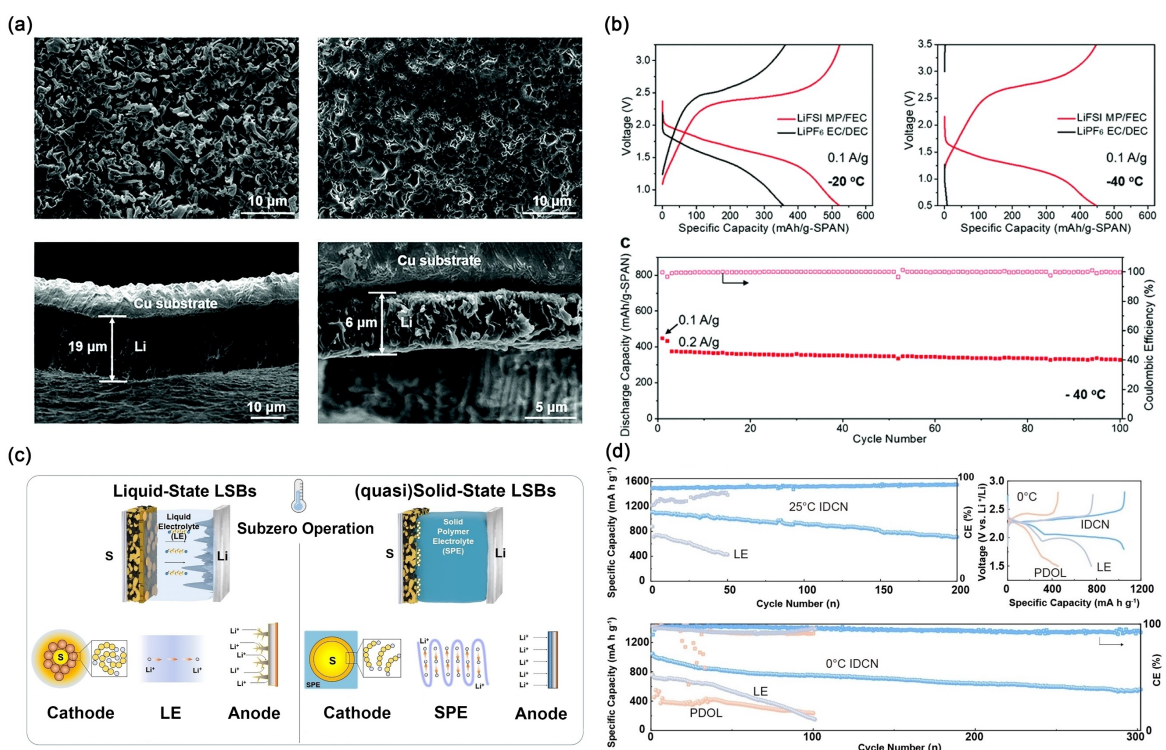


Figure 3. a) Top and cross-section views of SEM images of Li anode at 1 mAh cm^{-2} and 0.5 mA cm^{-2} circuit.^[49] b) Electrochemical performance in different electrolytes.^[49] c) Schematic illustrations comparing the LT operation of LSBs with liquid-state electrolyte and quasi-solid polymer electrolyte.^[50] d) Electrochemical performance for LSBs at different temperature.^[50]

expected to be used as a sulfur-equivalent electrode for high-multiplication and low-temperature all-solid-state batteries.

2.4. Improved Anode

Lithium metal's nucleation and deposition behavior at low temperatures is critical to cycling performance. McDowell et al.^[52] investigated lithium deposition/exfoliation, morphology evolution, and the structure and properties of the solid-electrolyte interphase (SEI) at temperatures as low as -80°C using an ether-based electrolyte (DOL/DME). The morphology of deposited lithium changed with decreasing temperature. The lithium-ion particles are smaller at lower temperatures, and this unique deposition morphology may lead to a large portion of the surface bare area and the formation of dead lithium. Zhang et al.^[53] demonstrated the nucleation and deposition behavior of lithium at low to ultra-low temperatures, and the use of dimethylsulfoxide (DMSO) as an electrolyte additive facilitated the nucleation of lithium and the construction of a robust solid electrolyte interface (SEI) layer on lithium-metal electrodes under icy conditions. Cryogenic transmission electron microscopy and X-ray photoelectron spectroscopy are used to characterize the microstructure and composition of the SEI. Electrochemical tests at temperatures as low as -80°C show that the SEI formed in the cold environment is resilient. Because the decomposition of lithium salts and solvents is a complex, multistep, and multi-electronic process, temperature affects the rate of each reaction and changes in the reaction products. Therefore, the thinner SEI formed at low temperatures is beneficial for stable battery cycling.^[54]

A summary of the literature on lithium-sulfur batteries shows that, with the decrease in ambient temperature, the charging voltage curve shows a non-linear change, and the proportion of the current charging stage decreases. When the ambient temperature is lower than a certain level, the voltage will instantly reach the charge cut-off voltage when charging the battery.^[55] The low-temperature discharge experiment of lithium-sulfur batteries shows that the discharge performance of the battery continues to deteriorate as the temperature decreases. In a low-temperature environment, the internal resistance of a lithium battery is proportional to the low temperature. Therefore, how to improve the low-temperature performance of lithium batteries is still a hot and difficult point of current research. The battery system reaction process mainly includes four steps: (1) Li^{+} transport in the electrolyte; (2) Li^{+} crossing the electrolyte/electrode interface membrane (3) charge transfer; and (4) Li^{+} diffusion in the active material body. At low temperatures, the rate of each step decreases, which causes the impedance of each step to increase, which leads to an increase in electrode polarization, and causes problems such as a decrease in low-temperature discharge capacity and lithium dendrites. To improve the low-temperature performance of lithium batteries, the influence of comprehensive factors, such as the positive electrode, negative electrode, and electrolyte in the battery, should be comprehensively considered. The electrolyte should be optimized; the positive

and negative materials should be modified to reduce the interface impedance.^[56]

3. Main Progress for High-Temperature Performances of Lithium-Sulfur Batteries

Li–S batteries perform poorly at high temperatures and have problems, such as lithium dendrite precipitation, electrolyte volatilization, and electrolyte decomposition, which must be addressed to improve the electrochemical behavior of Li–S batteries through comprehensive strategies.^[57] Although the rapidly increasing demand for electric vehicles, increased complexity of application conditions, longer operation time, and safety issues, especially flammability, are still the key factors determining the practical application of lithium-sulfur batteries. The safety of battery is closely related to the highly flammable diaphragm and liquid organic electrolyte.^[58] Moreover, high-temperatures also promote lithium polysulfide dissolution into the electrolyte, resulting in poor cycle life. High temperature Li–S batteries are seldom.^[59] Therefore, we have found relevant research on high-temperature lithium sulfur in recent years.^[60]

3.1. Improved Cathode

Hyea et al.^[61] reported the different temperature effects on the performance of Li–S batteries. Li–S button batteries were prepared by using S-permeated vertically aligned carbon nanotube arrays (S-CNT) as the cathode and lithium metal foil as the anode. The battery operated at 25, 50, 70 and 90°C (Figure 4a). Higher temperature operation leads to higher specific capacity, better rate capability and more stable performance. Higher conductivity of the SEI at higher temperatures likely counterbalanced its increased thickness and thus expectedly higher resistance, contributing to the high overall rate capability of the high-temperature cells. EDS and EIS studies reveal the main impact of temperature on the solid electrolyte interphase (SEI) on Li foil. Thicker SEI with higher content of inorganic phase formed at elevated temperatures greatly, which reduced the dendrite formation and the capacity fading resulting from the irreversible losses of S. At 70°C specific capacities up to $\sim 700 \text{ mAh g}^{-1}$ were achieved at an ultra-high current density of 3.3 A g^{-1} . At 90°C and with the same current density, Li–S cells showed an average capacity of $\sim 400 \text{ mAh g}^{-1}$ and stable performance for over 150 cycles. In addition to changing electrode materials, one possible solution to solve the temperature problems of lithium-sulfur batteries is to reuse traditional carbonate-based lithium-ion electrolytes, which promise practicable Li–S batteries for electric vehicles and other large-scale energy storage systems (Figure 4b). High-temperature Li–S batteries on universal carbon-sulfur electrodes by molecular layer deposited aglucone coating exhibit a safe and ultra-stable cycle life. researched by Li et al.^[62] In 2017, Chen et al.^[63] designed advanced sulfur hosts based on hybrid nanostructures of conductive polar materials and nanocarbons with high-rate

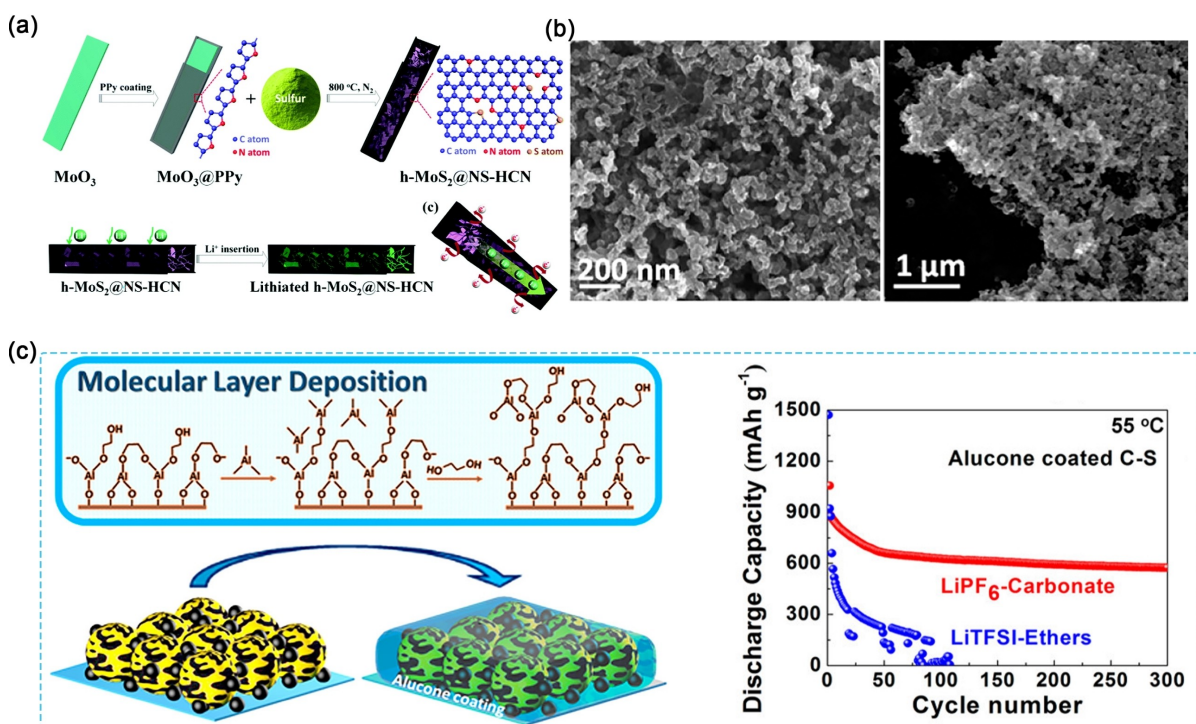


Figure 4. a) Schematic illustration of the formation of yolk-shelled MoS_2 @nitroge and electrochemical performance of high-temperature lithium-sulfur batteries.^[61] b) E-SEM images of alucone coated C-S electrode.^[62] c) Atomic layer deposition process on C-S electrodes and electrochemical performance of high-temperature lithium-sulfur batteries.^[62]

performance and heat resistance of Li–S batteries. Prepare interconnected carbon nanotubes were inserted into hollow Co_3S_4 nano boxes ($\text{CNTs}/\text{Co}_3\text{S}_4-\text{NB}_s$) as an efficient sulfur host material by self-templated. This design provided a micro-zoned and integrated three-dimensional conductive network, which significantly improves the utilization and rate performance of active sulfur. It can accelerate electron transmission and shortened the lithium-ion diffusion path, thereby promoting the kinetic behaviour of the electrochemical redox process. The electrode/electrolyte contact area was increased and more open channels were provided for electrolyte penetration. $\text{S}@\text{CNTs}/\text{Co}_3\text{S}_4-\text{NB}_s$ cathode material exhibited excellent high-rate performance.

In 2018, Lei et al.^[64] reported the researchers prepared a flame-retardant multifunctional membrane ($\text{PAN}@\text{APP}$) that effectively inhibits PS dissolution and high-temperature resistance through electrospun polyacrylonitrile (PAN) and ammonium polyphosphate (APP) for stability Safe lithium-sulfur battery (Figure 5a). Due to the abundant amine groups and phosphate contained in APP, $\text{PAN}@\text{APP}$ membrane has a strong binding effect with PS, which exerts a strong charge repulsion force to inhibit the conduction of negatively charged PS ions and free radicals. In addition, Refractory APP ensures the stability of the battery at high temperatures (Figure 5b). Using the $\text{PAN}@\text{APP}$ separator, the capacity retention rate of the Li–S battery during 800 cycles is 83%. Therefore, this kind of smart polymer separator shows potential application prospects in stabilizing safe batteries (Figure 5c-d).

Recently, Pu et al. developed Fe_3P electrocatalyst-assisted carbon-based sandwich-structured sulfur cathodes using a top-bottom strategy for high-rate and high-temperature Li–S batteries.^[65] The novel Fe_3P catalyst adsorbs most of the polysulfides and accelerates the corresponding conversion kinetics at the molecular level. When the battery's operating temperature was increased to 50 °C, a high reversible capacity of 1373 mA h g⁻¹ and ultra-stability of ~78.6% retention at 0.5 C was achieved (Figure 6a–b). Liu et al.^[66] synthesized poly-SCN, which can be reacted in ambient air at room temperature. The mild reaction conditions prevented thermally induced decomposition and led to high sulfur loading. In addition, poly-SCN synthesized by this method has a more uniform particle size distribution than poly-SCN synthesized mechanically. When applied as a cathode material in an ASSB with an operating temperature of 100 °C, the reversible capacity of poly-SCN exceeds 800 mA h g⁻¹, which is significantly better than that of elemental sulfur. Mechanistic studies show that when operated at these temperatures, poly-SCN undergoes a solid-solid reaction rather than the solid-liquid-solid reaction experienced by elemental sulfur. Poly-SCN synthesized by the SLR process represents a promising candidate for ASSBs designed for high-temperature applications (Figure 6c–d).

3.2. Electrolytes

The electrolyte is an essential part of the battery. The principal solvents DOL and DME in the traditional ether electrolyte have

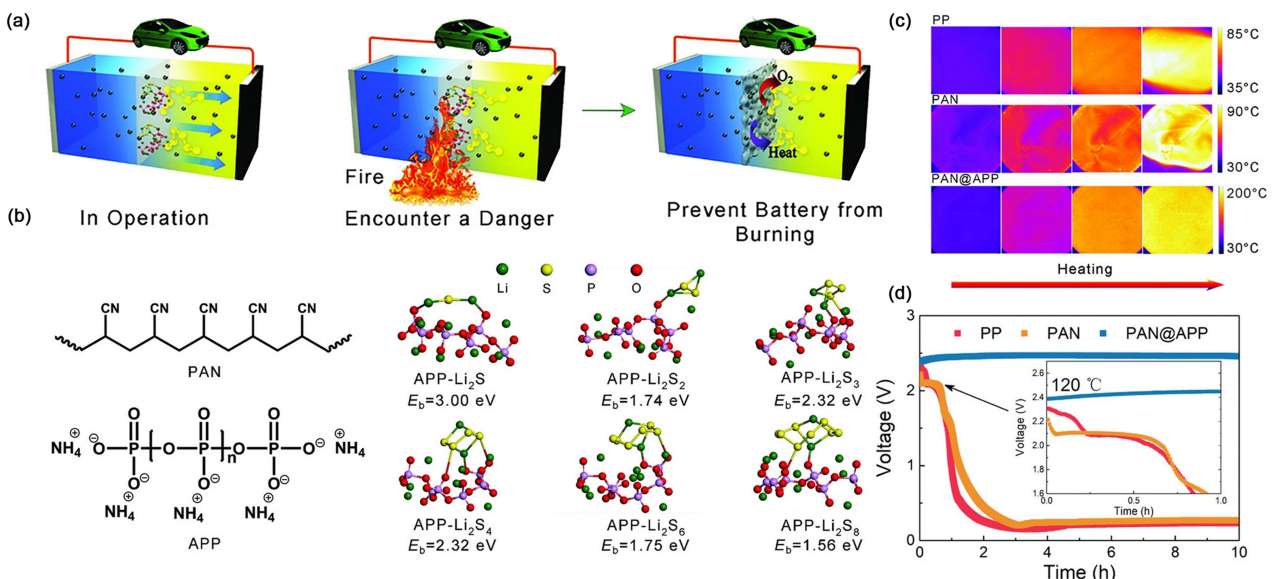


Figure 5. a) Schematics of the multifunctional electrospun separator with thermal-triggered flame-retardant properties for Li-S batteries. b) Schematics of Li₂S_x on APP, and binding energies for APP and Li-S composites c) Average thermograms of PP, PAN, and PAN@APP separators. d) Self-discharge behavior of different batteries at 120 °C.^[64]

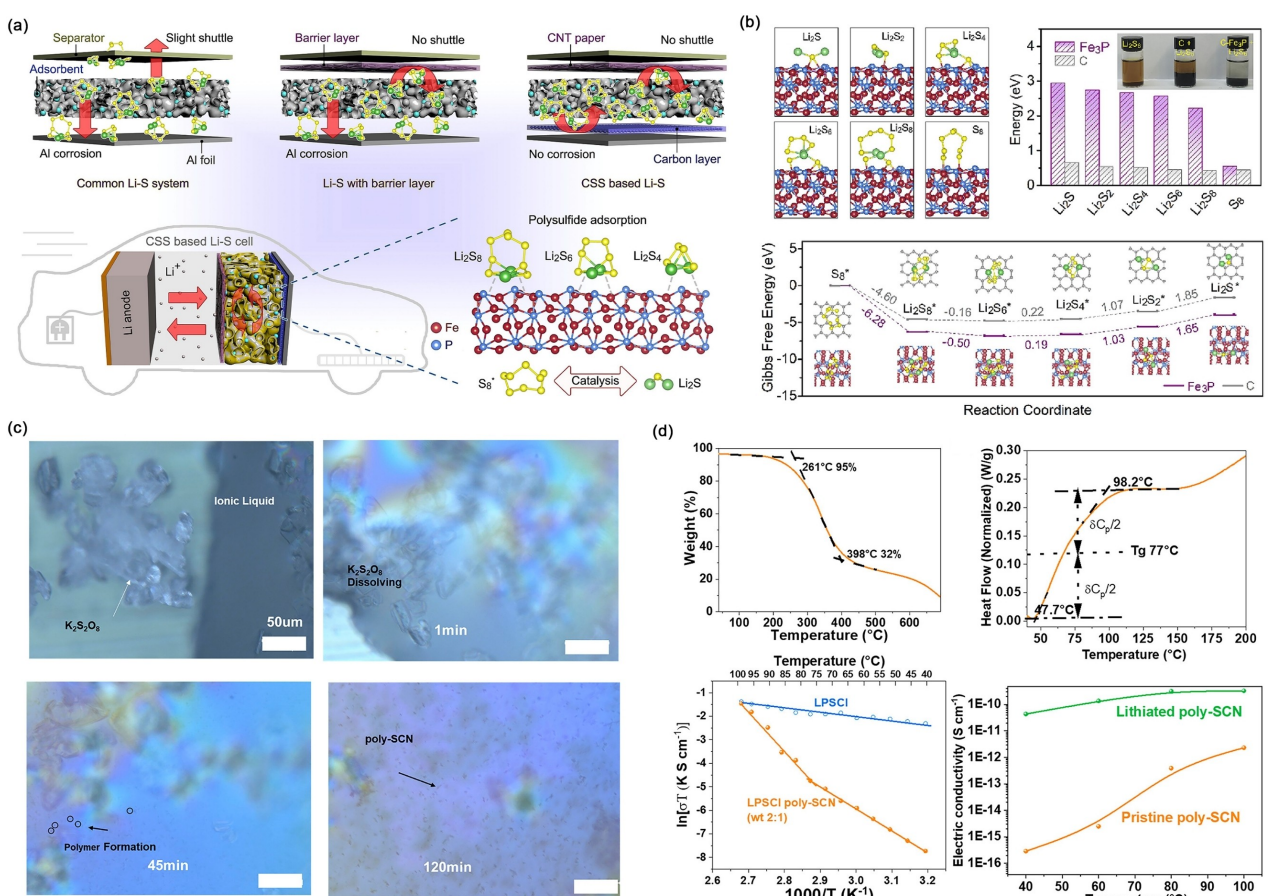


Figure 6. a) Diffusion of polysulfides and corrosion of Al current collector in different Li-S cathode systems.^[65] b) Synthesis procedure for polythiocyanogen (poly-SCN) by a solid-liquid reaction.^[66] c) Temperature-dependent properties of poly-SCN.^[66] d) Electrochemical properties of lithium-sulfur batteries.^[66]

low boiling points of 75 °C and 83 °C, respectively, making the solvents easy to volatilize. Therefore, using ether electrolytes in

high-temperature environments will cause serious safety problems. Currently, there are two main strategies for optimizing

ether electrolyte systems; the first is to replace the flammable ether solvents with ether solvents with higher boiling points and flash points to improve the stability of electrolytes. On the other hand, a flame retardant is added to the standard electrolyte for its safety. Wang et al.^[67] developed a flame-retardant electrolyte to enable extreme test conditions of using S@pPAN cathode at a high temperature (60 °C) (Figure 7a). He et al.^[68] solved the problems of shuttle effect and self-discharge by directly adding glutamic acid to the electrolyte. After adding glutamic acid, the negatively charged carboxylic acid group of glutamic acid effectively inhibited the polysulfide shuttle and ensures the efficient transport of Li⁺. The introduction of glutamic acid increased the stability of the traditional electrolyte at high temperatures and inhibited the self-discharge of lithium-sulfur batteries at high temperatures (Figure 7b). Cui et al.^[69] developed a nonflammable TDE electrolyte (dimethoxyether/1,1,2,2-tetrafluoroethyl 2,2,3,3-tetrafluoropropyl ether) with excellent flame retardancy and low solubility of polysulfides. In addition, a lithium-sulfur battery assembled with this flame-retardant electrolyte had a high discharge specific capacity of 870 mAh g⁻¹ at 60 °C. The assembled Li||Li symmetric battery can cycle for 2500 h at 1.0 mA cm⁻², confirming that the proposed flame-retardant electrolyte strategy could operate over a wide temperature range.

3.3. SEI Formation

A stable solid electrolyte interface (SEI) plays a crucial role in the cycle stability and coulomb efficiency (CE) of high-performance lithium-sulfur (Li–S) batteries. SEI film mainly comprises the elements C, O, F, Li and S. At higher temperatures, a thicker SEI layer was formed on the lithium metal anode. The high-temperature operation leads to thermal runaway in lithium-ion batteries, decomposition of conventional SEIs at >65 °C, and

the generation of large amounts of gas within the battery. Therefore, a stabilized SEI can protect the lithium metal anode from the continuous corrosion of the electrolyte at high temperatures, thus enhancing the thermal safety of lithium metal batteries. Over a duration period, extensive efforts are paid to the exploration of electrolyte additives for the interfacial stability by their sacrificial decomposition to form a robust SEI. Huang et al.^[70] proposed a surface-mediated method to pre-construct artificial SEIs on graphite surfaces. Dense and robust SEIs were constructed through free radical-induced polymerization and amide and sulfonate group decomposition. The constructed cells were capable of cycling for 200 cycles at 80 °C. This work is essential for the pre-formation of dense artificial SEI layers. However, the effect of soluble LiPSs on the structural components of SEI at both high temperatures needs to be further investigated (Figure 7c).

Lithium-sulfur batteries use sulfur materials for the positive electrode to improve the safety. However, there are still unsafe factors,^[71–73] such as the currently used electrolyte being flammable and the positive electrode material having low thermal stability during overcharge and under overcharge conditions. In an extreme environment, the battery will spontaneously generate heat inside. So far, the battery thermal stability and overcharge safety have improved, but research focuses on electrode materials and electrolytes. It is necessary to enhance lithium-ion diffusion,^[74–76] electronic conductivity, thermal stability, and flame retardancy of electrode materials, electrolytes, separators, and SEI layers to reduce heat generation and battery aging. Increasing the decomposition temperature of the SEI layer and the diaphragm can delay the internal short circuit and thermal runaway.^[77–79]

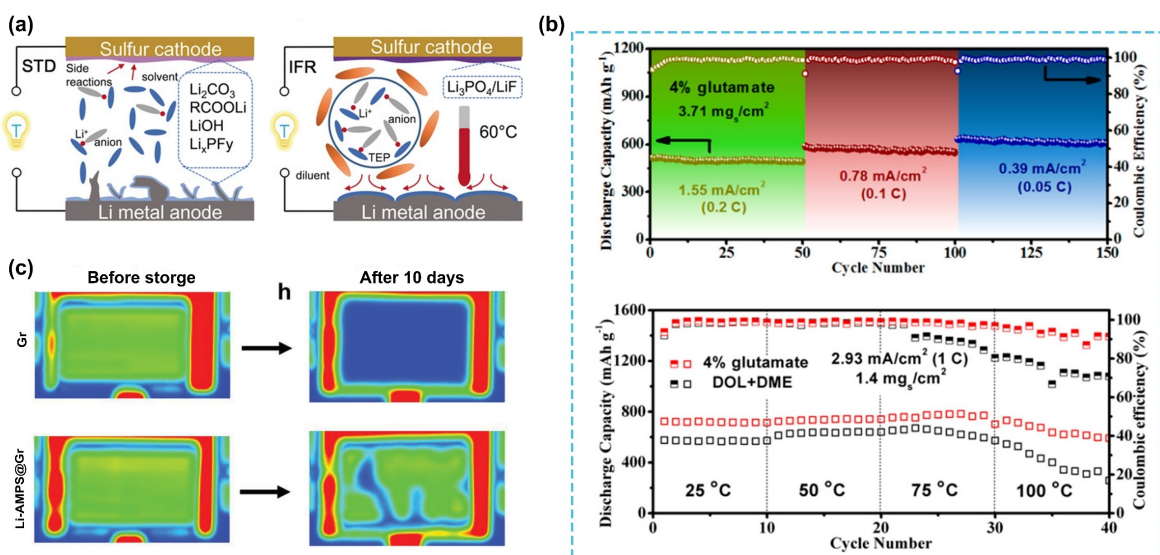


Figure 7. a) Illustration of Li@S batteries using STD electrolyte and IFR electrolyte.^[67] b) Electrochemical performance of lithium-sulfur batteries at different temperatures.^[68] c) Ultrasonic transmission mapping images of pouch cells before and after 10 days at 60 °C.^[70]

4. Main Progress for Wide-Temperature Performances of Lithium-Sulfur Batteries

Low and high-temperature environments present different challenges for conventional lithium-sulfur batteries. Under high-temperature conditions, the accelerated lithium ion diffusion rate leads to severe capacity degradation of lithium-sulfur batteries. At low temperatures, LiPSs aggregate and inhibit sulfur redox kinetics. Research has shown that wide-temperature lithium-sulfur batteries can be improved by optimizing electrodes, separators, and other vital materials.^[80] Some specific environmental occasions, such as the military, require some types of Li–S batteries with a wider operating temperature range. The operating temperature range is an important indicator of the power supply system; power supply systems carried by electric vehicles and military equipment should have a wide operating temperature range.^[81] The national military standard requires that the operating temperature range is –40~55 °C. The literature usually involves high-temperature and low-temperature performance, respectively, and there is very little research work on wide-temperature batteries. The relevant research on wide-temperature batteries will be reviewed from three aspects of cathode, electrolyte and anode.^[82]

4.1. Improved Cathode

The sluggish electrode kinetics of sulfur anode under wide-temperature conditions limit the commercial application of lithium-sulfur batteries. Compared with immobilizing lithium polysulfide on the surface of carrier materials, the introduction of various efficient catalytic components to accelerate the conversion of lithium polysulfide shows excellent potential in enhancing the electrochemical performance of lithium-sulfur batteries. Therefore, summarizing the intrinsic correlations in sulfur cathode is crucial for applying wide-temperature lithium-sulfur batteries. The wide-temperature range cathode material should be designed to meet the following conditions: 1) Ensure stable electrode/electrolyte interface. 2) Fast sulfur redox kinetics. 3) Stable CEI.

Sun et al.^[83] proposed a reactive bidirectional Fe₃C electrocatalyst collaboration strategy to achieve rapid and continuous sulfide conversion to improve the performance of Li–S batteries significantly. Ultimately, high area capacity Li–S cells (> 6.0 mAh cm⁻²) were operated stably over a wide temperature range (–10 to 40 °C). The strategy we developed for coupling reactive Li₂S with bi-directional electrocatalysts provides a new way to realize high-energy and wide-temperature Li–S batteries. Ma et al.^[84] design of polydendritic vanadium nitride as a catalyst to catalyze the conversion reaction of lithium polysulfide. In situ Raman spectroscopic characterization revealed that multidendritic vanadium nitride can significantly inhibit the shuttle effect of lithium polysulfide when used as a catalyst. Electrochemical tests showed that the lithium-sulfur battery could still work normally in the temperature range of –20 to

60 °C with high cycling stability. To present, restricted carbonaceous frameworks and electrode/electrolyte additives have been used, as well as the deployment of chemical catalysis to mitigate their solvation and shuttling effects. However, the attention has been not paid to controlling the precipitation of solid Li₂S₂/Li₂S. The irreversible precipitation of Li₂S₂/Li₂S not only leads to the loss of active material but also results in large charging overpotentials that block charge transfer pathways in the anode, thus reducing the utilization and practical capacity of the sulfur electrode. Li et al.^[85] proposed a sulfur electrode consisting of a lithium thiophosphate complex capable of binding and storing discharge reaction products without precipitation. In addition, the highly reversible all-liquid electrochemical conversion achieved excellent low-temperature cell workability (> 400 mAh g⁻¹ at –40 °C and > 200 mAh g⁻¹ at –60 °C). This work had opened new avenues for designing and customizing sulfur electrodes for enhanced electrochemical performance over a wide operating temperature range (Figure 8a–b). Wang et al.^[86] proposed a novel nanocomposite electrocatalyst (Ni@C/CNT) for wide-temperature Li–S batteries. The Ni@C/CNT electrocatalysts were then coated on commercial diaphragms as polysulfide traps and kinetic promoters. The modified LSBs can be stably operated in an ultra-wide temperature range from –50 °C to 70 °C, showing excellent ultra-wide temperature operating performance (Figure 8c–d). The critical parameters of wide-temperature Li–S batteries are shown in Table 2.

4.2. Electrolytes

Conventional ether-based electrolytes have low boiling and flash points, facilitating low-temperature applications. In order to expand the operating temperature window, researchers have devoted significant efforts to exploring novel lithium salts, concentrated electrolytes, and developing solid-state electrolytes. Cui et al. developed a concentrated flame-retarded concentrated electrolyte (6.5 m LiTFSI/FEC). A LiF-rich solid electrolyte interface was constructed on the lithium metal anode surface, enabling an extremely stable lithium stripping/plating process. Lithium-sulfur batteries with this concentrated electrolyte could have performed better at 90 °C and –10 °C.^[110] (Figure 9a). In conventional 1,2-dimethoxyethane (DME)-based electrolytes, the ordered macroporous cathode structure combined with bipartite binding sites ensures good ion transport, significantly improves sulfur redox kinetics, and effectively limits polysulfide shuttle effects. However, conventional DME-based electrolytes are intrinsically poorly stabilized with lithium metal, thus severely limiting the cycling stability of lithium-sulfur batteries, especially under extreme temperature conditions. Therefore, Zhao et al.^[111] improved electrode stability in extreme environments by combining selenium-doped S materials with high-fluorometer (HFE)-based electrolytes and revealed the underlying mechanism through in-situ characterization.(Figure 9b–c). All-solid-state lithium batteries are recognized as a new generation of battery technology. The “solid-solid” contact between the solid electrolyte and the active material limits the

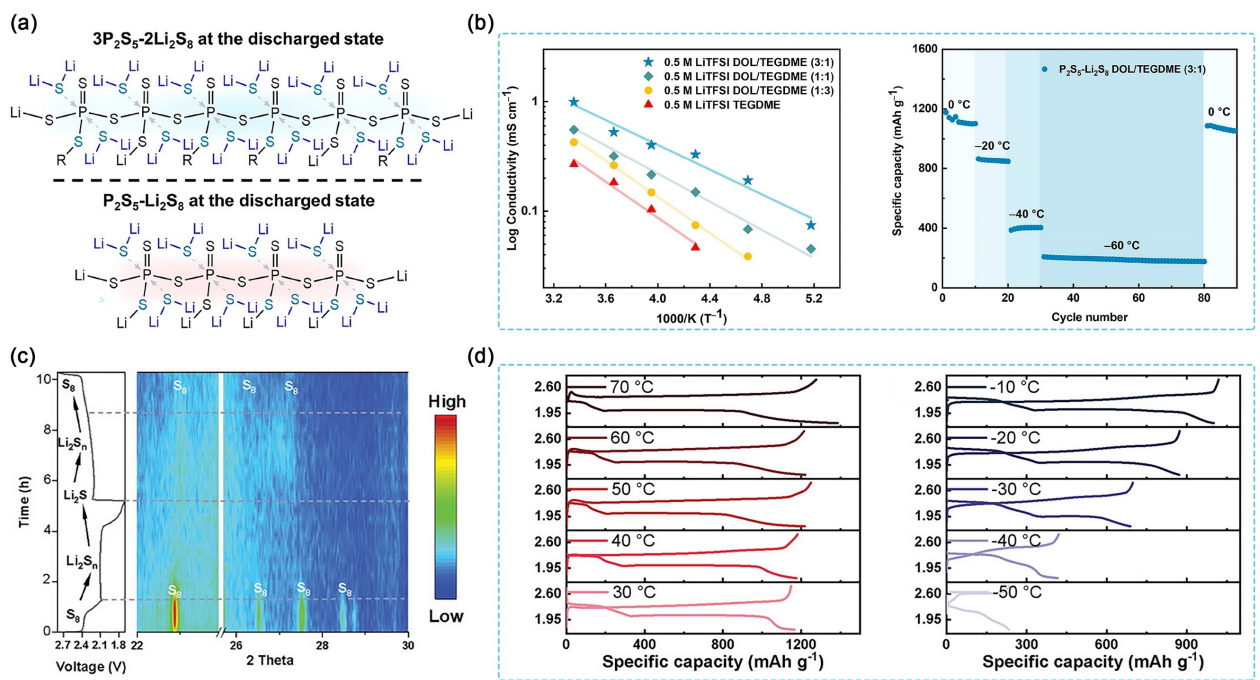


Figure 8. a) Proposed molecular structures of complexes at the discharged state (top: sixatom phosphorus unit structure associated with the $3\text{P}_2\text{S}_5\text{-}2\text{Li}_2\text{S}_8$ complex.^[85] b) Low-temperature battery performance evaluation.^[85] c) Top-view configuration of Li_2Sn adsorption on Ni atom surface. Contour maps of in situ X-ray diffraction (XRD) and corresponding discharge/charge profiles for the cell with $\text{Ni}@\text{C/CNT}$.^[86] d) Discharge/charge curves from 30 °C to 70 °C at 2 C.^[86]

Table 2. Key parameters of wide temperature lithium-sulfur battery.

Temperature-range	Cathode	Electrolyte	Temperature/°C	Current density	Capacity/mAh g ⁻¹	Reference
Low Temperature		LiTFSI-2CPME-2TTE	-20	0.2/0.5 C		87
	$\text{P}_2\text{S}_5\text{-Li}_2\text{S}_8$	DOL/TEGDME	-40	0.1 C	405	88
	$\text{TiO}_2@\text{C@CS}$		-20	0.1 C	136	89
	FCN-MO@CNFs		-40	0.2 C	1167.5	90
	$\text{Li}_2\text{S}_6/\text{FeCoNi}@C$		-40	0.2 C	785.0	91
	KB-S	0.1 M Electrolytes	-20	0.1 C	711	92
	CoFe@C@CNF		-20	0.2 C	836	93
		6.5 M LiTFSI in FEC	-10	0.1 C	453.4	94
		80% FDE-LAGP	-5	0.1 C	339	95
	GO-Zn(II)-AmT		-20	0.5 C	315	96
High Temperature	SPAN	2.5 M LiTFSI/tTPOS	80	1 C	760	97
		W-VO ₂ /PP	50	0.2		98
	CSS		50	0.5 C	1373	99
	$\text{WO}_3\text{-WS}_2$		90	7.0 A g ⁻¹		100
		DNA-CNT/MXene/PP	75	1 C	79% capacity retention	101
		$\text{Li}_{6.4}\text{La}_3\text{Zr}_{1.4}\text{Ta}_{0.6}\text{O}_{12}\text{TO}$	180	0.5 C	1287.9	102
	HCE-TTE		60	0.2 C	666	103
		TDE	60		870	104
	CON/CNT		0~65	5.0 C	625	105
	MB-VN		-20~60	1 C	678	106
Wide Temperature	PLG		0~60	0.2 C	516	107
		$\text{Ni-VO}_2/\text{PP}$	0~60		700	108
	3DC@S		-40~60	0.1 C	1072.5	109

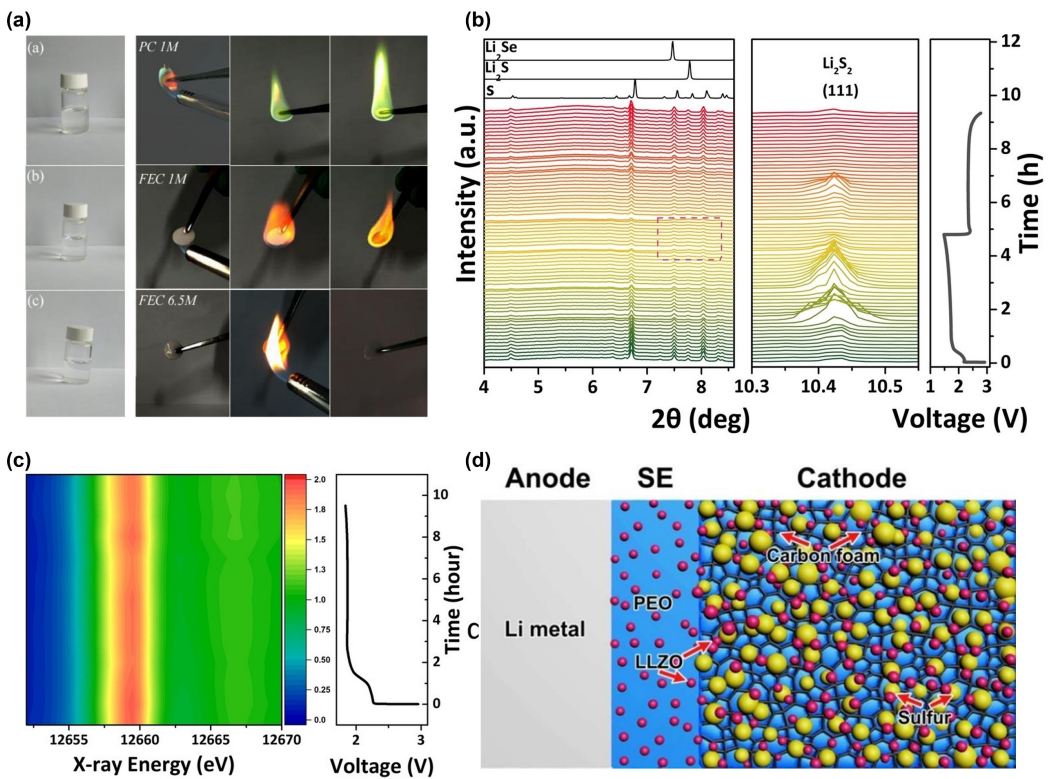


Figure 9. a) Flame-retardant photographs of 1 M LiDFOB/PC, 1 M LiTFSI/FEC and 6.5 M LiTFSI/FEC.^[110] b) Pushing Lithium-Sulfur Batteries towards Practical Working Conditions through a Cathode-Electrolyte Synergy.^[111] c) Discharge curve of OMSH–Se/S cathode at 0.1 C in HFE-based electrolyte and the corresponding in situ XANES spectra.^[111] d) Schematic illustration of an all solid-state Li–S battery based on LLZO nanostructures.^[112]

ion/electron transfer capability. As a result, poor ion-transport kinetics limits the performance of all-solid-state lithium-sulfur batteries at a wide range of temperatures. Cui et al.^[112] prepared Al³⁺/Nb⁵⁺ co-doped cubic Li₇La₃Zr₂O₁₂ (LLZO) nanoparticles and LLZO nanoparticle-modified porous foamed carbon (LLZO@C). The LLZO nanoparticle-filled PEO electrolyte had high ionic conductivity. The LLZO@C cathode-based lithium-sulfur batteries exhibited specific capacities of 1210 and 1556 mAh g⁻¹ at 50 °C and 70 °C, respectively. This study provides a promising strategy for constructing high-performance lithium-sulfur batteries in a wide temperature range (Figure 9d).

4.3. Improved Anode

The stable operation and cycle life of lithium-sulfur batteries depend mainly on the reversibility of the sulfur cathode and lithium metal anode. Strategies of reliable lithium metal anodes have been extensively explored, including electrolyte structure tuning, SEI layer design, and anode material optimization. A specific review of Li-anode optimization has been reported. The behavior of Li metal in different temperature environments has been scarcely reported. Cui et al.^[113] demonstrated that high-temperature battery operation can produce favorable SEI nanostructures that provide faster kinetics, improving CE and cycling stability. In DOL/DME/LiNO₃ electrolyte, the CE was as high as 99.8% and remained stable over 300 cycles. Low-temperature

electron microscopy (Cryo-EM) characterization revealed the formation of an organic/inorganic composite layered SEI at 60 °C, which was different from the amorphous polymer SEI formed at 20 °C. This emerging SEI maintains mechanical stability during cycling and effectively passivates the lithium surface, resulting in long-term cycling stability. Wang et al.^[114] explored the temperature-dependent nucleation and growth behavior of lithium by increasing the temperature from 20 °C to 60 °C to construct a dendrite-free lithium metal anode. Significant effects of temperature on the nucleation behavior and electrochemical properties of lithium metal anode were found. The high lithium-ion mobility at high temperatures contributes to the formation of a lithium deposition layer. The excellent performance of Li||LTO full battery at 60 °C exceeded that at 20 °C. Therefore, increasing the temperature is an efficient and straightforward method to develop high-performance lithium metal-based batteries. Robert W et al. demonstrated that external thermal gradients profoundly affected the plating and stripping stability of lithium-metal batteries, potentially providing a way to produce safe, rechargeable lithium-metal batteries. Symmetric lithium-metal interfaces with negative thermal gradients (0 °C cathode, 40 °C anode) had high resistance and limit lithium-ion transport at the electrode surface. Forming a uniform initial electrodeposition at the positive thermal gradient (40 °C cathode, 0 °C anode) made the battery easy to stabilize for long-term cycling. The positive thermal gradient reduced harmful electrode-electrolyte reactions, decreased the

formation of electrochemically inactive lithium, and maintained a low bending diffusion pathway for higher ionic conductivity and lower interfacial resistance. Moreover, it demonstrates that a positive thermal gradient as an operational strategy is expected to charge lithium metal anode batteries faster.^[115]

5. Summary and Outlook

Lithium-sulfur batteries with ultra-high theoretical energy density (2600 Wh kg^{-1}) have received much attention. Many literatures reported that the stable cycling of lithium-sulfur batteries at room temperature can be improved by optimizing the electrodes and electrolytes. However, the capacity of lithium-sulfur batteries is severely degraded under extreme temperature conditions, hindering the commercialization of lithium-sulfur batteries. Commercial batteries are typically required to operate in temperatures ranging from $-30\text{--}70^\circ\text{C}$. In addition, to meet the needs of aerospace or military applications, it is essential to extend the operating temperature range of lithium-sulfur batteries (below -50°C or above 100°C). At high temperatures, the “shuttle effect” of LiPSs and the safety of the electrolyte are more severe problems. At low temperatures, the conversion kinetics of LiPSs are slow, and the anode passivation is severe, resulting in high ion diffusion resistance. By systematically reviewing the recent reports on LiPSs in different temperature ranges, we propose the following promising solutions for designing wide-temperature LiPSs.

5.1. Low-Temperature Lithium-Sulfur Batteries

The resistance at electrode-electrolyte interfaces at low temperatures will significantly increase due to the sluggish charge transfer kinetics of LiPSs conversion. Designing electrode structures with fast adsorption-catalysis and multidimensional ionic pathways is an effective strategy to solve the above problems. The addition of appropriate additives can reduce the viscosity and freezing point of the electrolyte and decrease the electrode/electrolyte interface resistance. In addition, the conductivity of electrode materials, coating thickness, pore structure, and other factors also affect the low-temperature performance of lithium-sulfur batteries. However, more advanced characterization techniques are needed to reveal the polysulfide conversion process at low temperatures.

5.2. High-Temperature Lithium-Sulfur Batteries

Compared to room-temperature batteries, the high-temperature lithium-sulfur batteries have safety issues, such as severe shuttle effects of LiPSs and thermal instability of ether-based electrolytes. When lithium-sulfur batteries reach high temperatures, the highest occupied molecular orbitals (HOMO) and the lowest unoccupied molecular orbitals (LUMO) are also displaced with increasing temperature. When the HOMO of the electrolyte is higher than the cathodic potential (μ_c), electrons are easily

transferred from the electrolyte to the cathodic active material, causing oxidation of the electrolyte. Therefore, the thermal stability of the electrolyte is directly related to the safety of the battery in a high-temperature environment. The multifunctional additives into the electrolyte can be considered to regulate the Li^+ solvation configuration, which can reduce the desolvation energy barrier. Considering the severe side reactions at high temperatures, it becomes crucial to introduce highly selective catalytic materials into lithium-sulfur cathodes.

5.3. Wide-Temperature Lithium-Sulfur Batteries

The wide-temperature performance of lithium-sulfur batteries is related to electrolytes and electrodes. Introducing many negatively charged functional additives (e.g., glutamic acid) into the electrolyte can inhibit the shuttle effect of polysulfides. In addition, inorganic and liquid small molecules can be added to the sulfur cathode as catalytic materials to improve sulfur redox kinetics. On the anode side, the significant loss of active lithium leads to low coulombic efficiency, which hinders the practical operation of lithium-metal batteries over a wide temperature range. Therefore, constructing alloy anodes can effectively improve the cycle life of lithium-sulfur batteries in a wide-temperature environment.

5.4. Perspectives and Challenge

This review comprehensively explains the advances, challenges, and future research directions on wide-temperature lithium-sulfur batteries. The processability of sulfur-containing cathode materials, advanced electrolytes, and lithium metal anodes at extreme temperatures are thoroughly analyzed. The primary challenges of lithium-sulfur batteries in developing a wide-temperature range are high and low-temperature conditions for polysulfide shuttling and conversion, flammable and unstable electrolytes, and inhomogeneous SEI. To address the above challenges, researchers have successfully proposed various strategies, such as designing high-performance cathode materials, developing non-flammable electrolytes, constructing novel electrodes, and constructing artificial SEI layers. Although wide-temperature lithium-sulfur battery performance has improved significantly, it still falls short of commercialized performance standards. Therefore, further utilization of in-situ characterization techniques, machine learning algorithms, and the advancement of solid-state electrolytes should be pursued to optimize the mechanism and enhance the performance of wide-temperature batteries.

Acknowledgements

We acknowledge the funding support from the Harbin Manufacturing Science and Technology Innovation Talent Project [2022CXRCCG007], Heilongjiang Province Ecological

Environment Protection Research Project [HST2022DQ007] and the National Natural Science Foundation of China [21706043].

Conflict of Interests

The authors declare no conflict of interest.

Data Availability Statement

The data that support the findings of this study are available from the corresponding author upon reasonable request.

Keywords: Lithium sulfur • Wide temperature • Critical material • Electrochemistry

- [1] S. Jin, X. Gao, S. Hong, Y. Deng, P. Chen, R. Yang, Y. Lak Joo, L. A. Archer, *JOUL* **2024**, DOI: 10.1016/j.joule.2023.12.022.
- [2] Y. Gao, X. Nan, R. Zhao, B. Sun, W. Xu, Q. Li, Y. Cong, Y. Li, W. Lv, Q. Zhang, X. Li, N. Yang, *Adv. Funct. Mater.* **2023**, 24, 2310117.
- [3] J. S. Park, C. H. Jo, S. T. Myung, *Energy Storage Mater.* **2023**, 61, 102869.
- [4] X. Xiao, L. Wang, Y. Wu, Y. Song, Z. Chen, X. He, *Energy Environ. Sci.* **2023**, 16, 2856–2868.
- [5] J. Liu, Y. Zhang, J. Zhou, Z. Wang, P. Zhu, Y. Cao, Y. Zheng, X. Zhou, C. Yan, T. Qian, *Adv. Funct. Mater.* **2023**, 33, 2302055.
- [6] X. Chen, L. Li, Y. Shan, D. Zhou, W. Cui, Y. Zhao, *J. Energy Chem.* **2022**, 70, 502–510.
- [7] J. Liu, Y. Cao, J. Zhou, M. Wang, H. Chen, T. Yang, Y. Sun, T. Qian, C. Yan, *ACS Appl. Mater. Interfaces* **2020**, 12, 54537–54544.
- [8] K. Li, Y. Li, W. Shen, Y. Zhang, X. Qu, J. Huang, G. Yang, Y. Lin, *Int. J. Therm. Sci.* **2024**, 198, 108880.
- [9] H. Su, H. Yang, C. Ma, J. Tang, C. Zhu, X. Wang, D. Zeng, *ACS Sens.* **2024**, DOI: 10.1021/acssensors.3c02230.
- [10] T. Zhao, P. Xiao, S. Nie, M. Luo, M. Zou, Y. Chen, *Coord. Chem. Rev.* **2024**, 502, 215592.
- [11] Y. Hang, L. Li, Y. Shan, Y. Zhao, S. Fan, *Appl. Surf. Sci.* **2023**, 635, 157738.
- [12] J. Y. Maeng, M. Bae, Y. Kim, D. Kim, Y. Chang, S. Park, J. Choi, E. Lee, J. Lee, Y. Piao, *J. Mater. Chem. A* **2024**, 12, 1058–1071.
- [13] L. B. Li, Y. H. Shan, *New Carbon Mater.* **2021**, 36, 336–349.
- [14] H. Chen, J. Liu, X. Zhou, H. Ji, S. Liu, M. Wang, T. Qian, C. Yan, *Chem. Eng. J.* **2021**, 404, 126470.
- [15] Z. Xiao, D. Han, Y. Fu, K. Xie, W. Tian, C. Shu, K. Xi, C. Peng, Y. Wu, S. Dou, W. Tang, *Chem. Eng. J.* **2024**, 480, 148029.
- [16] Y. Zhang, J. Zhang, Z. Ding, L. Zhang, L. Deng, L. Yao, H. Y. Yang, *ACS Nano* **2023**, 17, 25519–25531.
- [17] T. Kim, *Nano Energy* **2024**, 120, 109711.
- [18] A. Raulo, G. Jalilvand, *Nano Energy* **2024**, 12, 109265.
- [19] F. Pei, L. Wu, Y. Zhang, Y. Liao, Q. Kang, Y. Han, H. Zhang, Y. Shen, H. Xu, Z. Li, Y. Huang, *Nat. Commun.* **2024**, 15, 351.
- [20] B. Qi, X. Hong, Y. Jiang, J. Shi, M. Zhang, W. Yan, C. Lai, *Nano-Micro Lett.* **2024**, 16, 71.
- [21] Q. Li, J. Chen, S. Zhang, R. Liu, X. Jiang, Z. Zhang, C. Wang, L. Yin, R. Wang, *Energy Storage Mater.* **2024**, 65, 103138.
- [22] C. Liu, C. Mo, L. Zhong, X. Gong, Y. Zhang, X. Wang, F. Yang, J. Li, J. Lu, D. Yu, *Angew. Chem. Int. Ed.* **2023**, 62, 202312016–202312025.
- [23] Y. X. Yin, S. Xin, Y. G. Guo, L. J. Wan, *Angew. Chem. Int. Ed.* **2013**, 52, 13186–13200.
- [24] A. Manthiram, Y. Fu, S. H. Chung, C. Zu, Y.-S. Su, *Chem. Rev.* **2014**, 114, 11751–11787.
- [25] D. Li, J. Liu, N. Xu, M. Wang, X. Liu, T. Yang, T. Qian, C. Yan, *New J. Chem.* **2019**, 43, 15267–15274.
- [26] Y. H. Shan, L. B. Li, J. T. Du, M. Zhai, *New J. Chem.* **2021**, 36, 1094–1101.
- [27] J. Feng, C. Shi, H. Dong, C. Zhang, W. Liu, Y. Liu, T. Wang, X. Zhao, S. Chen, J. Song, *J. Energy Chem.* **2023**, 86, 135–145.
- [28] J. Zhou, S. Qian, B. Hao, J. Liu, X. Zhou, C. Yan, T. Qian, *Adv. Funct. Mater.* **2023**, 33, 2213966.
- [29] Z. Wang, Y. Li, H. Ji, J. Zhou, T. Qian, C. Yan, *Adv. Mater.* **2022**, 34, 2203699.
- [30] M. L. Divya, Y. S. Lee, V. Aravindan, *Batteries & Supercaps* **2022**, 5, e202200214.
- [31] J. Zhou, S. Qian, B. Hao, J. Liu, X. Zhou, C. Yan, T. Qian, *Adv. Funct. Mater.* **2023**, 33, 2213966.
- [32] X. Su, X. P. Xu, Z. Q. Ji, J. Wu, F. Ma, L. Z. Fan, *Electrochim. Energy Rev.* **2024**, 7, 2.
- [33] G. Hasegawa, N. Kuwata, T. Ohnishi, K. Takada, *J. Mater. Chem. A* **2024**, 12, 731–738.
- [34] M. Li, M. Floetenmeyer, E. Bryant, E. Cooper, S. Tao, R. Knibbe, *ACS Appl. Mater. Interfaces* **2023**, 46, 53333–53341.
- [35] Z. Li, Y. Ren, X. Guo, *Mater. Chem. Front.* **2023**, 7, 6305–6317.
- [36] Z. Yao, Y. Wang, S. Wan, W. Ma, J. Rong, Y. Xiao, G. Hou, S. Chen, *Mater. Chem. Front.* **2023**, 7, 6061–6084.
- [37] Y. V. Mikhaylik, J. R. Akridge, *J. Electrochem. Soc.* **2023**, 150, A306.
- [38] H. S. Ryu, H. J. Ahn, K. W. Kim, J. H. Ahn, K. K. Cho, T. H. Nam, J. U. Kim, G. B. Cho, *J. Power Sources* **2006**, 163, 201–206.
- [39] Q. Tan, Z. Zhang, X. Wen, G. Fang, S. Xu, Z. Nie, Y. Wang, *Appl. Energy* **2024**, 358, 122610.
- [40] B. Zhao, C. Zhou, P. Chen, X. Gao, *ACS Appl. Interfaces* **2024**, 16, 4679–4688.
- [41] J. Ding, W. Wang, Y. Zhang, H. Mu, X. Cai, Z. Chang, G. Wang, *Phys. Chem. Chem. Phys.* **2024**, 26, 6316–6324.
- [42] P. Tan, Y. Yin, D. Cai, B. Fei, C. Zhang, Q. Chen, H. Zhan, *J. Mater. Chem. A* **2024**, 12, 3711–3721.
- [43] S. Zhu, Y. Wang, J. Jiang, X. Yan, D. Sun, Y. Jin, C. Nan, H. Munakata, K. Kanamura, *ACS Appl. Mater. Interfaces* **2016**, 27, 17253–17259.
- [44] Z. Zhang, Y. Wang, J. Liu, D. Sun, X. Ma, Y. Jin, Y. Cui, *Electrochim. Acta* **2018**, 271, 58–66.
- [45] N. Gao, Y. Zhang, C. Chen, B. Li, W. Li, H. Lu, L. Yu, S. Zheng, B. Wang, *J. Mater. Chem. A* **2022**, 10, 8378–8389.
- [46] H. Ji, Z. Wang, Y. Sun, Y. Zhou, S. Li, J. Zhou, T. Qian, C. Yan, *Adv. Mater.* **2023**, 35, 2208590.
- [47] Z. Guan, X. Chen, F. Chu, R. Deng, S. Wang, J. Liu, F. Wu, *Adv. Energy Mater.* **2023**, 13, 2302850.
- [48] Y. Zhao, L. Huang, D. Zhao, J. Lee, *Angew. Chem. Int. Ed.* **2023**, 62, e202308976.
- [49] G. Cai, J. Holoubek, D. Xia, M. Li, Y. Yin, X. Xing, P. Liu, Z. Chen, *Chem. Commun.* **2020**, 56, 9114–9117.
- [50] J. Zhang, J. Chou, X. X. Luo, Y. M. Yang, M. Y. Yan, D. Jia, C. H. Zhang, Y. H. Wang, W. P. Wang, S. J. Tan, J. C. Guo, Y. Zhao, F. Wang, S. Xin, L. J. Wan, Y. G. Guo, *Angew. Chem. Int. Ed.* **2023**, 13, e202316087.
- [51] P. Lu, S. Gong, F. Guo, X. Zhu, Y. Huang, Y. Wang, W. He, M. Yang, L. Chen, H. Li, F. Wu, *Nano Energy* **2023**, 118, 109029.
- [52] A. C. Thenuwara, P. Shetty, M. McDowell, *Nano Lett.* **2019**, 19, 8664–8672.
- [53] Y. Zhang, J. Luo, C. Wang, X. Hu, E. Matios, W. Li, *Mater. Chem. Front.* **2022**, 6, 1405–1413.
- [54] L. Wu, J. Hu, S. Chen, X. Yang, L. Liu, J. Foord, P. Pobedinskas, K. Haenen, H. Hou, J. Yang, *Electrochim. Acta* **2023**, 466, 142973.
- [55] R. Gao, M. Zhang, Z. Han, X. Xiao, X. Wu, Z. Piao, Z. Lao, L. Nie, S. Wang, G. Zhou, *Adv. Mater.* **2024**, 36, 2303610.
- [56] W. Chen, T. Lei, C. Wu, M. Deng, C. Gong, K. Hu, Y. Ma, L. Dai, W. Lv, W. He, X. Liu, J. Xiong, C. Yan, *Chem. Eng. J.* **2018**, 8, 1702348.
- [57] P. Lyu, X. Liu, J. Qu, J. Zhao, Y. Huo, Z. Qu, Z. Rao, *Energy Storage Mater.* **2020**, 31, 195–220.
- [58] Y. Wang, Y. Zhang, H. Cheng, Z. Ni, Y. Wang, G. Xia, X. Li, X. Zeng, *Molecules* **2021**, 26, 1535.
- [59] G. Zhu, K. Wen, W. Lv, X. Zhou, Y. Liang, F. Yang, Z. Chen, M. Zou, J. Li, Y. Zhang, W. He, *J. Power Sources* **2015**, 300, 29–40.
- [60] L. Lu, X. Han, J. Li, J. Hua, M. Ouyang, *J. Power Sources* **2013**, 15, 272–288.
- [61] Y. Liu, J. Zhu, J. Xu, S. Liu, L. Li, C. Zhang, T. Liu, *Nanoscale* **2018**, 10, 7536–7543.
- [62] X. Li, A. Lushington, Q. Sun, W. Xiao, J. Liu, B. Wang, Y. Ye, K. Nie, Y. Hu, Q. Xiao, R. Li, J. Guo, T. K. Sham, X. Sun, *Nano Lett.* **2016**, 16, 3545–3549.
- [63] T. Chen, Z. Zhang, B. Cheng, R. Chen, Y. Hu, L. Ma, G. Zhu, J. Liu, Z. Jin, *J. Am. Chem. Soc.* **2017**, 139, 12710–12715.
- [64] T. Lei, W. Chen, Y. Hu, W. Lv, X. Lv, Y. Yan, J. Huang, Y. Jiao, J. Chu, C. Yan, C. Wu, Q. Li, W. He, J. Xiong, *Adv. Energy Mater.* **2018**, 8, 1802441.
- [65] J. Pu, Y. Tan, Z. Wang, Z. Fang, P. Xue, Y. Yao, *Chem. Eng. J.* **2023**, 471, 144374.

- [66] S. Wang, J. Zhou, S. Feng, M. Patel, B. Lu, W. Li, C. Soulen, J. Feng, Y. S. Meng, P. Liu, *ACS Energy Lett.* **2023**, *8*, 2699–2706.
- [67] H. Ma, Q. Wang, H. Lu, Y. Si, X. Kong, J. Wang, *Angew. Chem. Int. Ed.* **2019**, *58*, 791–795.
- [68] L. Dong, J. Liu, D. Chen, Y. Han, Y. Liang, M. Yang, C. Yang, W. He, *ACS Nano* **2019**, *13*, 14172–14181.
- [69] B. Tang, H. Wu, X. Du, X. heng, X. Liu, Z. Yu, J. Yang, M. Zhang, J. Zhang, G. Cui, *Small* **2020**, *16*, 1905737.
- [70] X. Zheng, Z. Cao, W. Luo, T. Zhao, Y. Han, H. Yang, X. Liu, Y. Zhou, J. Wen, Y. Shen, H. Zheng, Y. Huang, *Adv. Funct. Mater.* **2023**, *33*, 2301550.
- [71] P. Lyu, X. Liu, J. Qu, J. Zhao, Y. Huo, Z. Qu, Z. Rao, *Energy Storage Mater.* **2020**, *31*, 195–220.
- [72] Q. Wang, L. Jiang, Y. Yu, J. Sun, *Nano Energy* **2019**, *55*, 93–114.
- [73] X. Huang, J. Xue, M. Xiao, S. Wang, Y. Li, S. Zhang, Y. Meng, *Energy Storage Mater.* **2020**, *30*, 87–97.
- [74] S. Wang, K. Rafiz, J. Liu, Y. Jin, J. Y. S. Lin, *Sustain. Energy Fuels* **2020**, *4*, 2342–2351.
- [75] Z. W. Seh, Y. Sun, Q. Zhang, Y. Cui, *Chem. Soc. Rev.* **2016**, *45*, 5605–5634.
- [76] Z. Du, Y. Kao, J. H. Park, *J. Franklin Inst.* **2020**, *357*, 121–141.
- [77] Q. Cheng, W. Xu, S. Qin, S. Das, T. Jin, A. Li, A. C. Li, B. Qie, P. Yao, H. Zhai, C. Shi, X. Yong, Y. Yang, *Angew. Chem. Int. Ed.* **2019**, *58*, 5557–5561.
- [78] S. Chen, J. Zheng, L. Yu, X. Ren, M. H. Engelhard, C. Niu, H. Lee, W. Xu, J. Xiao, J. Liu, J. G. Zhang, *JOUL* **2018**, *2*, 1548–1558.
- [79] Z. Li, W. Lu, N. Zhang, Q. Pan, Y. Chen, G. Xu, D. Zeng, Y. Zhang, W. Cai, M. Yang, Z. Yang, Y. Sun, H. Ke, H. Cheng, *J. Mater. Chem. A* **2018**, *6*, 14330–14338.
- [80] S. Meng, Y. Xie, W. Yan, D. Sun, Y. Jin, *J. Alloys Compd.* **2020**, *838*, 155517.
- [81] J. Liu, N. Nie, J. Wang, M. Hu, J. Zhang, M. Li, Y. Huang, *Mater. Today Energy* **2020**, *16*, 100372.
- [82] J. Liu, X. Li, J. Huang, G. Yang, J. Ma, *Adv. Funct. Mater.* **2024**, *2*, 2312762.
- [83] P. Zeng, C. Yuan, J. An, X. Yang, C. Cheng, T. Yan, G. Liu, T. S. Chan, J. Kang, L. Zhang, X. Sun, *Energy Storage Mater.* **2022**, *44*, 425–432.
- [84] L. Ma, Y. Wang, Z. Wang, J. Wang, Y. Cheng, J. Wu, B. Peng, J. Xu, W. Zhang, Z. Jin, *ACS Nano* **2023**, *17*, 11527–11536.
- [85] P. Wang, N. Kateris, B. Li, Y. Zhang, J. Luo, C. Wang, Y. Zhang, A. S. Jayaraman, X. Hu, H. Wang, W. Li, *J. Am. Chem. Soc.* **2023**, *145*, 18865–18876.
- [86] H. Zhang, J. Chen, Z. Li, Y. Peng, J. Xu, Y. Wang, *Adv. Funct. Mater.* **2023**, *33*, 2304433.
- [87] H. Zhang, Z. Zeng, Q. Wu, X. Wang, M. Qin, S. Lei, S. Cheng, J. Xie, *J. Energy Chem.* **2024**, *90*, 380–387.
- [88] P. Wang, N. Kateris, B. Li, Y. Zhang, J. Luo, C. Wang, Y. Zhang, A. S. Jayaraman, X. Hu, H. Wang, W. Li, *J. Am. Chem. Soc.* **2023**, *145*, 18865–18876.
- [89] J. Li, L. Liu, J. Wang, Y. Zhuang, B. Wang, S. Zhen, *ACS Sustainable Chem. Eng.* **2023**, *11*, 3657–3663.
- [90] X. Pang, B. An, S. Zheng, B. Wang, *Chem. Eng. J.* **2023**, *458*, 141445.
- [91] X. Pang, H. Geng, S. Dong, B. An, S. Zheng, B. Wang, *Small* **2023**, *19*, 2205525.
- [92] F. Chu, M. Wang, J. Liu, Z. Guan, H. Yu, B. Liu, F. Wu, *Adv. Funct. Mater.* **2022**, *32*, 2205393.
- [93] N. Gao, Y. Zhang, C. Chen, B. Li, W. Li, H. Lu, L. Yu, S. Zheng, B. Wang, *J. Mater. Chem. A* **2022**, *10*, 8378–8389.
- [94] J. Yu, J. Zhang, C. Wang, R. Hu, X. Du, B. Tang, H. Qu, H. Wu, X. Liu, X. Zhou, X. Yang, G. Cui, *J. Energy Chem.* **2020**, *51*, 154–160.
- [95] S. Gu, X. Huang, Q. Wang, J. Jin, Q. Wang, Z. Wen, R. Qian, *J. Mater. Chem. A* **2017**, *5*, 13971–13975.
- [96] Z. Zhang, Y. Wang, J. Liu, D. Sun, X. Ma, Y. Jin, Y. Cui, *Electrochim. Acta* **2018**, *271*, 58–66.
- [97] H. Ma, Q. Wang, H. Lu, Y. Si, X. Kong, J. Wang, *Chem. Eng. J.* **2024**, *479*, 14757.
- [98] G. Liu, Q. Zeng, S. Tian, X. Sun, D. Wang, Q. Wu, W. Wei, T. Wu, Y. Zhang, Y. Sheng, K. Tao, E. Xie, Z. Zhang, *Small* **2023**, *15*, 2307040.
- [99] J. Pu, Y. Tan, Z. Wang, Z. Fang, P. Xue, Y. Yao, *Chem. Eng. J.* **2023**, *471*, 144374.
- [100] Y. Li, Q. Zhang, S. Shen, S. Wang, L. Shi, D. Liu, Y. Fu, D. He, *Chem. Eng. J.* **2023**, *468*, 143562.
- [101] Y. Li, M. Li, Y. C. Zhu, S. Song, S. N. Li, J. Aarons, L. C. Tang, J. Bae, *Composites Part B* **2023**, *251*, 110465.
- [102] S. Wu, Y. Yao, X. Nie, Z. Yu, Y. Yu, F. Huang, *Small* **2022**, *18*, 2202651.
- [103] M. He, X. Li, N. G. Holmes, R. Li, J. Wang, G. Yin, P. Zuo, X. Sun, *ACS Appl. Mater. Interfaces* **2021**, *13*, 38296–38304.
- [104] B. Tang, H. Wu, X. Du, X. Cheng, X. Liu, Z. Yu, J. Yang, M. Zhang, J. Zhang, G. Cui, *Small* **2020**, *16*, 1905737.
- [105] A. Zhu, S. Li, Y. Yang, B. Peng, Y. Cheng, Q. Kang, Z. Zhuang, L. Ma, J. Xu, *Small* **2023**, *5*, 2305494.
- [106] L. Ma, Y. Wang, Z. Wang, J. Wang, Y. Cheng, J. Wu, B. Peng, J. Xu, W. Zhang, Z. Jin, *ACS Nano* **2023**, *17*, 11527–11536.
- [107] C. Li, Q. Sun, Q. Zhang, C. Xu, S. Wang, Y. Ma, X. Shi, H. Zhang, D. Song, L. Zhang, *Chem. Eng. J.* **2023**, *455*, 140706.
- [108] D. Zhang, R. Gu, F. Y. Lan, W. Y. Guo, C. W. Deng, Q. J. Xu, H. X. Li, Y. L. Min, *ACS Sustainable Chem. Eng.* **2021**, *9*, 16251–16261.
- [109] C. Hai, G. Peng, Y. Zhou, Y. Shen, X. Li, Y. Sun, G. Zhang, J. Zeng, S. Dong, *Ceram. Int.* **2022**, *48*, 1622–1632.
- [110] Z. Yu, J. Zhang, C. Wang, R. Hu, X. Du, B. Tang, H. Qu, H. Wu, X. Liu, X. Zhou, X. Yang, G. Cui, *J. Energy Chem.* **2020**, *51*, 154–160.
- [111] C. Zhao, A. Daali, I. Hwang, T. Li, X. Huang, D. Robertson, Z. Yang, S. Trask, W. Xu, C. J. Sun, G. L. Xu, K. Amine, *Angew. Chem. Int. Ed.* **2022**, *61*, e202203466.
- [112] X. Tao, Y. Liu, W. Liu, G. Zhou, J. Zhao, D. Lin, C. Zu, O. Sheng, W. Zhang, H.-W. Lee, Y. Cui, *Nano Lett.* **2017**, *17*, 2967–2972.
- [113] J. Wang, W. Huang, A. Pei, Y. Li, F. Shi, X. Yu, Y. Cui, *Nat. Energy* **2019**, *4*, 664–670.
- [114] N. Li, Q. Ye, K. Zhang, H. Yan, C. Shen, B. Wei, K. Xie, *Angew. Chem. Int. Ed.* **2019**, *58*, 18246–18251.
- [115] R. Atkinson, R. Carter, C. Love, *Energy Storage Mater.* **2019**, *22*, 18–28.

Manuscript received: January 20, 2024

Revised manuscript received: February 17, 2024

Accepted manuscript online: February 29, 2024

Version of record online: March 19, 2024